ARTICLE   **OPEN**

Check for updates

Stroboscopic high-order nonlinearity for quantum optomechanics

Andrey A. Rakhubovsky [1]✉ and Radim Filip [1]

High-order quantum nonlinearity is an important prerequisite for the advanced quantum technology leading to universal quantum processing with large information capacity of continuous variables. Levitated optomechanics, a field where motion of dielectric particles is driven by precisely controlled tweezer beams, is capable of attaining the required nonlinearity via engineered potential landscapes of mechanical motion. Importantly, to achieve nonlinear quantum effects, the evolution caused by the free motion of mechanics and thermal decoherence have to be suppressed. For this purpose, we devise a method of stroboscopic application of a highly nonlinear potential to a mechanical oscillator that leads to the motional quantum non-Gaussian states exhibiting nonclassical negative Wigner function and squeezing of a nonlinear combination of mechanical quadratures. We test the method numerically by analyzing highly instable cubic potential with relevant experimental parameters of the levitated optomechanics, prove its feasibility within reach, and propose an experimental test. The method paves a road for experiments instantaneously transforming a ground state of mechanical oscillators to applicable nonclassical states by nonlinear optical force.

npj Quantum Information (2021)7:120 ; https://doi.org/10.1038/s41534-021-00453-8

INTRODUCTION

Quantum physics and technology with continuous variables (CVs)[1] has achieved noticeable progress recently. A potential advantage of CVs is the in-principle unlimited energy and information capacity of a single oscillator mode. In order to fully gain the benefits of CVs and to achieve *universal* quantum processing one requires an access to a nonlinear operation[2,3], that is, at least a cubic potential. In addition, the CV quantum information processing can be greatly simplified and stabilized if variable higher-order potentials are available[4]. Variability of nonlinear gates can also help to overcome limits for fault tolerance[5]. Nanomechanical systems profit from a straightforward feasible way to achieve the nonlinearity by inducing a controllable classical nonlinear force of electromagnetic nature on a linear mechanical oscillator[6–8]. Such a nonlinear force needs to be fast, strong, and controllable on demand to access different nonlinearities required for an efficient universal CV quantum processing. Therefore, the field of optomechanics[9–12] is a promising candidate to provide the key element for the variable *on-demand* nonlinearity. Optomechanical systems have reached a truly quantum domain recently, demonstrating the effects ranging from the ground state cooling[13,14] and squeezing[15,16] of the mechanical motion to the entanglement of distant mechanical oscillators[17,18]. Of particular interest are the levitated systems in which the potential landscape of the mechanical motion is provided by a highly developed device—an optical tweezer[19–22]. Levitated systems have proved useful in force sensing[23,24], studies of quantum thermodynamics[25–27], testing fundamental physics[28–30], and probing quantum gravity[31,32]. From the technical point of view, the levitated systems have recently demonstrated noticeable progress in the controllability and engineering, particularly, cooling toward[33–36] and eventually reaching the motional ground state[37]. Further theoretical studies of preparation of entangled states of levitated nanoparticles are underway[38,39]. Besides the inherently nonlinear optomechanical interaction met in the standard bulk optomechanical systems the levitated ones possess the attractive possibility of engineering the nonlinear trapping potential[26,37,40–44].

Moreover, the trapping potentials can be made time-dependent and manipulated at rates exceeding the rate of mechanical decoherence and even the mechanical frequency[45]. In this manuscript, we assume a similar possibility to generate the nonlinear potential for a mechanical motion and control it in a fast way (faster than the mechanical frequency). Our findings do not rely on the specific method of how the nonlinearity is created.

Here we propose a broadly applicable nonlinear stroboscopic method to achieve high-order nonlinearity in optomechanical systems with time- and space-variable external force. The method builds on the possibility to control the nonlinear part of the mechanical potential landscape and introduce it periodically, adjusted in time with the mechanical harmonic oscillations. Such periodic application inhibits the effect of the free motion and the restoring force terms in the Hamiltonian and allows approaching the state arising from the nonlinear potential only. This is achieved similarly to how a stroboscopic measurement enables a quantum nondemolition detection of displacement[46,47]. To prove feasibility of the method, we theoretically investigate realistic dynamics of a levitated nanoparticle in the presence of simultaneously a harmonic and a strong, stroboscopically applied, nonlinear potentials enabled by the engineering of the trapping beam. To run numerical simulations, we advance the theory of optomechanical systems beyond the covariance matrix formalism appropriate for Gaussian states. Using direct Fock-basis and Suzuki-Trotter[48] simulations we model the simultaneous action of the nonlinear potential and harmonic trap, and obtain the Wigner functions (WFs) of the quantum motional states achievable in this system. We predict very nonclassical negative WFs[49,50] generated by highly nonlinear quantum-mechanical evolution for time shorter than one mechanical period. The oscillations of WF reaching negative values, in accordance with estimates based on unitary dynamics, witness that the overall quantum state undergoes unitary transformation $\exp(iV(\hat{x})\tau)$ sufficient for universal quantum processing[2]. To justify it, we prove a nonlinear combination of the canonical quadratures of the mechanical oscillator to be

---

[1]Department of Optics, Palacký University, Olomouc, Czech Republic. ✉email: andrey.rakhubovsky@gmail.com

A.A. Rakhubovsky and R. Filip

squeezed below the ground state variance which is an important prerequisite of this state being a resource for the measurement-based quantum computation[51,52]. For numerical simulations, we focus our attention to realistic version of the key nonlinearity, namely the cubic one with $V(x) \propto x^3$, and find good agreement of the predictions based on experimentally feasible dynamics with the lossless and noiseless unitary approximation. The method allows straightforward extension to more complex nonlinear potentials which can be used for flexible generation of other resources for nonlinear gates and their applications[4,52]. In comparison with simultaneously developed superconducting quantum circuits[53], an advantage of our approach stems from a much larger flexibility of nonlinear potentials. Stroboscopic driving of an optomechanical cavity in a linear regime was considered in ref. [54] for the purpose of cooling and Gaussian squeezing of the mechanical mode.

RESULTS

The nonlinear stroboscopic protocol

To implement the stroboscopic method, it is possible to versatilely use a levitated nanoparticle[45] with optical[6], electric[7] or magnetic[8] trapping. It is also possible to use a mirror equipped with a fully optical spring[55], or a membrane with electrodes allowing its nonlinear actuation and driving[56]. In any of such systems, the mechanical mode can be posed into nonlinear potential $V(x)$, particularly, the cubic potential $V_3(x) \propto x^3$ for the pioneering test. In this manuscript, we focus on the experimental parameters peculiar to the levitated nanoparticles[36,37], although the principal results remain valid for the other systems as well. We also focus here solely on the evolution of the mechanical mode of the optomechanical cavity, assuming that the coupling to the optical cavity mode (blue in Fig. 1) is switched off.

The mechanical mode is a harmonic oscillator of eigenfrequency Ω_m, described by position and momentum quadratures, respectively, $\hat{x}$ and $\hat{p}$, normalized such that $[\hat{x}, \hat{p}] = 2i$. The oscillator is coupled to a thermal bath at rate η_m. We also assume fast stroboscopic application of an external nonlinear potential $a(t)$
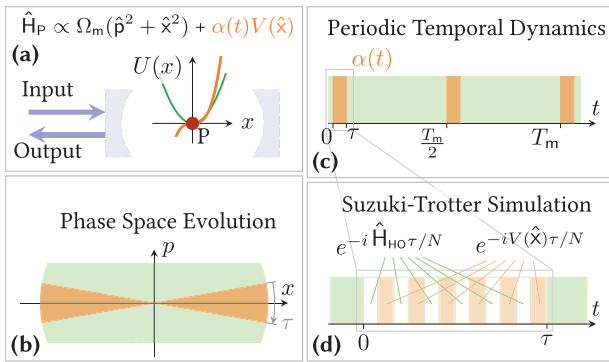

Fig. 1 **Scheme of the proposed stroboscopic method. a** A levitated optomechanical system as an illustration of mechanical oscillator in a nonlinear potential. A dielectric subwavelength particle (P) is trapped by a tweezer (not shown). The particle feels a total potential $U(x) = \Omega_m x^2/4 + a(t)V(x)$ that is a sum of the quadratic (green) and the nonlinear (orange, here: cubic) parts, both provided by the trapping beam. The particle can be placed inside a high-Q cavity and probed by the laser light. **b, c** Stroboscopic application of nonlinear potential. The nonlinear part of the potential is switched on for only a short fraction of the mechanical period (orange segments). The quadratic trapping potential (green segments) is present throughout all the evolution. **d** Suzuki-Trotter simulation of stroboscopic evolution of the mechanical mode. In the figure, orange segments represent action of the nonlinear potential, empty and filled green segments correspond, respectively, to unitary and damped harmonic evolution.

$V(x)$ with a piecewise constant $a(t)$ illustrating the possibility to periodically switch the nonlinear potential on and off as depicted at Fig. 1(a). The Hamiltonian of the system, therefore, reads ($\hbar = 1$)

$$\hat{H} = \hat{H}_{HO} + a(t)V(\hat{x}), \quad \hat{H}_{HO} = \frac{1}{4}\Omega_m(\hat{x}^2 + \hat{p}^2), \tag{1}$$

To illustrate the key idea behind the stroboscopic method, we first examine the regime of absent mechanical damping and decoherence. In this case, the unitary evolution of the oscillator is given by $\rho(t) = \hat{U}(t, t_0)\rho(t_0)\hat{U}^\dagger(t, t_0)$, with $\hat{U}(t + \delta t, t) = \exp[-i\hat{H}\delta t]$. When the nonlinearity is switched on permanently ($a(t) = a_0$), the free evolution dictated by H_{HO} mixes the quadratures of the oscillator which prohibits the resulting state from possessing properties of the target nonlinear quantum state arising purely from $V(x)$ regardless of the nonlinearity strength (see Supplementary Note 4 for more details). Willing to obtain a unitary transformation as close to $\exp[-iV(\hat{x})\tau]$ as possible despite a constant presence of $\hat{H}_{HO}$, we assume that the nonlinearity is repeatedly switched on for infinitesimally short intervals of duration τ. If the duration τ is sufficiently short for the harmonic evolution to be negligible, the resulting evolution during τ is approximately purely caused by the $V(x)$ part of the Hamiltonian. To enhance the magnitude of the effect of the nonlinear potential, $V(\hat{x})$ we can apply it every $2\pi/\Omega_m$ for short enough intervals as shown in Fig. 1b, c) . This allows to establish an effective rotating frame within which the nonlinearity is protected from the effect of harmonic evolution. Realistically, the stroboscopic application corresponds to $a(t) = \sum_k \delta_\tau(t - 2\pi k/\Omega_m)$, with $k \in \mathbb{Z}$, where δ_τ is a physical approximation of Dirac delta function with width τ much shorter than the period of mechanical oscillations: $\tau\Omega_m \ll 1$. Then we can consider the evolution over a number M of harmonic oscillations as consisting of subsequent either purely harmonic or purely nonlinear steps, and the evolution operator can be approximately written as

$$\hat{U}(t + MT_m, t) = [\hat{U}(t + T_m, t)]^M \approx \left\{ \exp[-i\hat{H}_{HO}T_m] \exp[-iV(\hat{x})\tau] \right\}^M$$
$$= \exp[-iMV(\hat{x})\tau]. \tag{2}$$

For the last equality we used the fact that the unitary harmonic evolution through a single period of oscillations is an identity map: $\hat{U}_{HO}(t + T_m, t) \equiv \exp[-i\hat{H}_{HO}T_m] = \hat{\mathbb{1}}$. Motion of a real mechanical oscillator can be approximated by a harmonic unitary evolution with good precision because of very high quality of mechanical modes of optomechanical systems[35,36,57]. Equation (2) shows that the effect of sufficiently short pulses of the strong nonlinear potential timed to be turned on precisely once per a period of mechanical oscillations M times, is equivalent to an M-fold increase of the nonlinearity.

A further improvement is possible by noting that undamped harmonic evolution over a half period simply flips the sign of the two quadratures $(\hat{x}, \hat{p}) \mapsto -(\hat{x}, \hat{p})$. Therefore, it is possible to similarly apply the potential twice per period, switching its sign each second time. This can be formalized as setting $a(t) = \sum_k (-1)^k \delta_\tau(t - \pi k/\Omega_m)$, $k \in \mathbb{Z}$. In this case,

$$\hat{U}(t + T_m, t) = e^{-i\hat{H}_{HO}T_m/2}e^{+iV(\hat{x})\tau}e^{-i\hat{H}_{HO}T_m/2}e^{-iV(\hat{x})\tau} = e^{-2iV(\hat{x})\tau}, \tag{3}$$

and therefore, after M periods

$$\hat{U}(t + MT_m, t) = \exp[-i \cdot 2M \cdot V(\hat{x})\tau]. \tag{4}$$

The idealized scheme proposed above in reality faces two potentially deteriorative factors: the finiteness of the duration of the nonlinearity τ, and the mechanical decoherence caused by the thermal environment. We take a proper account of these two

factors by considering the evolution as consisting of two kinds: (i) unitary undamped dynamics in a sum of the quadratic and nonlinear potentials, (ii) damped harmonic evolution between those. These two kinds of evolution are subsequently repeated, as shown in Fig. 1b, c. We develop an advanced method based on Suzuki-Trotter simulation (STS) to simulate the quantum state of a realistic optomechanical system after the application of our proposed protocol. It is worth noting that the STS is typically used to approximately achieve a novel evolution $\hat{U}$ from experimentally available exact unitaries[58,59]. In our work, we use STS to simulate and justify that the experimentally available compound evolution $\hat{U}$ can approximate one of its building blocks $\hat{U}_{NL}(\delta t) \equiv \exp(-iV(x)\delta t)$. To verify the convergence of STS we also perform simulations in the Fock-state basis that allow direct computation of the propagator corresponding to the Hamiltonian (1). Fock-state-basis simulations unfortunately do not grant access to phase-space distributions such as WF[60] which makes use of STS the primary strategy. Excellent agreement between the very distinct methods (STS and Fock-state-basis simulations) indicates that our results are correct. The details of the simulation methods are presented in Supplementary Notes 1 and 2.

We omit damping and thermal decoherence during the fast unitary action of the combined potential. Such applications are assumed to happen every half of a mechanical oscillation and have durations much shorter than the mechanical period, therefore, due to high quality of state-of-the-art mechanical oscillators, such omission is justified. The joint action is simulated using STS and verified by Fock-state-basis simulation. Between the applications of the nonlinear potential $V(x)$ the mechanical oscillator experiences damped harmonic evolution described by the linear Heisenberg-Langevin equations

$$\dot{x} = \Omega_m p; \quad \dot{p} = -\Omega_m x - \eta_m p + \sqrt{2\eta_m}\xi, \tag{5}$$

where ξ is the quantum Langevin force, obeying $[\xi(t), x(t)] = i\sqrt{2\eta_m}$ and $\frac{1}{2}\langle\{\xi(t), \xi(t')\}\rangle = (2n_{th} + 1)\delta(t - t')$ with n_{th} being the mean occupation of the bath. The experimentally accessible value of the heating rate H_m is given by $H_m = \eta_m n_{th}$. The density matrix $\rho(T_m/2)$ of the particle after half of a period of oscillations including the action of the nonlinear potential and subsequent damping can be formally written as

$$\rho(\tau) = \mathcal{N}[\rho(0)] = \mathcal{D}\left[\hat{U}(\tau, 0)\rho(0)\hat{U}^\dagger(\tau, 0)\right]. \tag{6}$$

where $\hat{U}(\tau, 0)$ describes the particle's unitary dynamics in combined potential, and $\mathcal{D}[\bullet]$ indicates the mapping performed by the damping. Generalization of (6) to include the second half of the period, and the subsequent generalization to multiple periods, is straightforward.

Using these advanced numerical tools, further elaborated in "Methods" we evaluate the quantum state of the mechanical oscillator after the protocol and explore the limits of the achievable nonlinearities in the optomechanical systems that are accessible now or are within reach.

Application to the cubic nonlinearity
Motivated by the role of cubic nonlinearity for the universal continuous-variable quantum processing, we illustrate the devised method by numerically evaluating the evolution of a levitated particle under a stroboscopic application of a cubic potential $V(x) \propto x^3$. The nonlinear phase gate $e^{-iV(x)}$ is a limit case of motion, it modifies only momentum of the object without any change of its position. This nondemolition aspect is crucial for use in universal quantum processing. A nonlinear phase state (particularly, the cubic phase state introduced in[3]) as the outcome of evolution of the momentum eigenstate $|p = 0\rangle$ in a nonlinear potential $V(x)$ is

defined as

$$|\gamma_V\rangle \propto \int dx \, e^{iV(x)\tau}|x\rangle, \tag{7}$$

where $V(x)$, is a highly nonlinear potential, and $|x\rangle$ the position eigenstate $\hat{x}|x\rangle = x$. The state (7) requires an infinite squeezing possessed by the ideal momentum eigenstate before the nonlinear potential is applied. More physical is an approximation of this state obtained from a finitely squeezed thermal state $\rho_0(r, n_0)$, ideally, vacuum, by the application of V:

$$\rho(V, r, n_0) = e^{iV(\hat{x})\tau}\rho_0(r, n_0)e^{-iV(\hat{x})\tau}. \tag{8}$$

The initial state ρ_0 is the result of squeezing a thermal state with initial occupation n_0

$$\rho_0(r, n_0) = \hat{S}(r)\rho_0(0, n_0)\hat{S}^\dagger(r) \tag{9}$$

where $\hat{S}(r) = \exp[\frac{1}{2}r^*(\hat{a})^2 - \frac{1}{2}r(\hat{a}^\dagger)^2]$ is a squeezing operator $(\hat{a} = (\hat{x} + i\hat{p})/2)$, and the initial state ρ_0 is thermal with mean occupation n_0. Phase of the squeezing parameter $r = |r|e^{i\theta}$ determines the squeezing direction. When $n_0 = 0$, $|r| \to +\infty$, and $\theta = \pi$, the initial state is infinitely squeezed in p, and Eq. (8) approaches the ideal cubic state (7).

The quantum state obtained as a result of the considered sequence of interactions approximates the ideal state given by Eq. (7). The quality of the approximation can be assessed by evaluating the variance of a nonlinear quadrature $p - \lambda x^2$, or the cuts of the WFs of the states. A reduction in nonlinear quadrature variance below the vacuum is a necessary condition for application of these states in nonlinear circuits[51,52]. On the other hand, the phase-space interference fringes of the WF reaching negative values are a very sensitive witness of quantum non-Gaussianity of the states used in the recent experiments[61–64]. Fidelity happens to be an improper measure of the success of the preparation of the quantum resource state[65] because it does not predict either applicability of these states as resources or their highly nonclassical aspects.

A noise reduction in the cubic phase gate can be a relevant first experimental test of the quality of our method. The approximate cubic state obtained from a squeezed thermal state (that is, the state (8) with $V(x) = \gamma x^3/(6\tau)$) should possess arbitrary high squeezing in the variable $p - \lambda x^2$ for $n_0 = 0$ given sufficient squeezing of the initial mechanical state. The state (8) obtained from a squeezed in momentum state, has the following variance of the nonlinear quadrature

$$\sigma_3^\rho(\lambda) \equiv \text{Tr}(\rho(\hat{p} - \lambda\hat{x}^2)^2) - \left(\text{Tr}\rho(\hat{p} - \lambda\hat{x}^2)\right)^2 = \frac{v_{th}}{s^2} + 2(\lambda - \gamma)^2\left(s^2 v_{th}\right)^2, \tag{10}$$

where $v_{th} = 2n_0 + 1$ is the variance of each canonical quadrature in the initial thermal state before squeezing, and $s = e^r$ is the magnitude of squeezing. An important threshold is the variance of the nonlinear quadrature attained at the vacuum state ($n_0 = 0$, $s = 1$)

$$\sigma_3^{vac}(\lambda) = 1 + 2\lambda^2. \tag{11}$$

Application of a unitary cubic evolution to the initial vacuum state displaces this curve along the λ axis by γ. Further, as follows from Eq. (10), squeezing the initial state allows reducing the minimal value of σ_3, and increase of the initial occupation n_0 causes also increase of σ_3. Suppression of fluctuations in the nonlinear quadrature is a convenient figure of merit because it is a direct witness of the applicability of the quantum state as a resource for measurement-based quantum information processing[51,52] and a witness of non-classicallity[66]. It can be evaluated in an optomechanical system with feasible parameters using pulsed optomechanical interaction[66] without a full quantum state tomography.
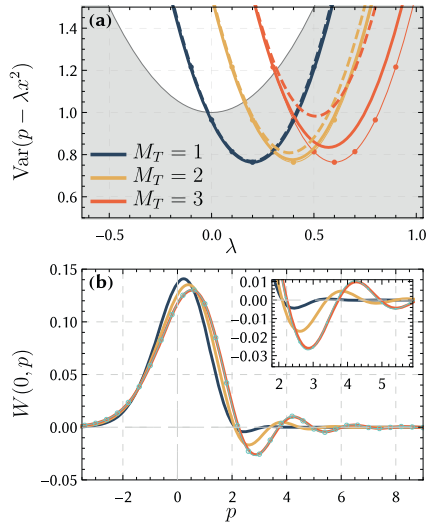
Fig. 2 Results of the simulations. Results of stroboscopic application of cubic nonlinear potential $V = \gamma x^3/(6\tau)$ to the squeezed thermal state (initial occupation $n_0 = 0.05$, squeezing $s = 1.2$) over multiple ($M_T = 1, 2,$ or 3) halves of mechanical periods. **a** Squeezing of nonlinear quadrature. Thick lines correspond to stroboscopic method with realistic parameters and thermal noise, thin lines, to purely unitary application of the nonlinearity. Dashed lines correspond to the result of evolution driven by the full Hamiltonian $\hat{H}$ (1) from the same initial state over time τ, 2τ, and 3τ respectively. **b** Wigner function of motional states. Solid lines correspond to the same states from (**a**). Cyan line with markers (overlapping with solid red line) shows the unitary application of nonlinearity. Other parameters are as follows: potential stiffness $\gamma = \gamma_0 = 0.2$, application duration $\tau\Omega_m = \Theta = \Theta_0 = \pi/100$, environmental thermal heating rate parameter $H_0 = 4\pi H_m/\Omega_m = 0.002$.

In Fig. 2a, we show the variance σ_3 at the instants $t = M_T T_m/2$. Each of the curves takes into account also the interaction with the thermal environment lasting $T_m/2$ after each application of the nonlinearity. The heating rate parameter $H_0 = 4\pi H_m/\Omega_m$ assumes value $H_0 = 2 \times 10^{-3}$. For an oscillator of eigenfrequency $\Omega_m = 2\pi \times 100$ kHz and $Q = 10^6$ is equivalent to occupation of the environment equal to $n_{th} \approx 10^7$ phonons. This is the equilibrium occupation of such an oscillator at the temperature of 50 K. A recent experiment of ground state cooling of a levitated nanoparticle[37] reported the heating rate corresponding to $H \approx 10^2 H_0$. A proof of robustness of the method against such heating is in the Supplementary Note 3.

Thin lines with markers show the analytic curves defined by Eq. (10) for the corresponding values of γ. The good quantitative correspondence between the approximate states resulting from the realistic stroboscopic application of nonlinear potential and the analytic curves again proves the validity of the stroboscopic method. Importantly, each of the curves has an area where it lies below the corresponding ground-state level $\sigma_3$vac. This means each of the corresponding states gives advantage over vacuum if used as ancilla for the cubic gate. The dashed lines show the simulated quantum states obtained from the same initial state by longer unitary evolution according to the full Hamiltonian from Eq. (1), that is $e^{-iHn\tau}\rho e^{iHn\tau}$ where $n = 1, 2, 3$ for blue, yellow and red correspondingly. Further divergence from ideal than that of the ones corresponding to the stroboscopic method witnesses an advantage of the latter in generation of the resource for the measurement-based computation.

The stroboscopic application of a fixed limited gain nonlinearity, therefore, indeed allows amplification of nonlinearity in accordance with Eq. (4). Importantly, even despite requiring longer

evolution in a noisy environment, the stroboscopic method allows better amplification than a unitary longer application of the nonlinearity in presence of the free evolution ($\propto \hat{p}^2$) and harmonic ($\propto \hat{x}^2$) terms in the Hamiltonian.

The non-Gaussian character of the prepared quantum state can be witnessed via its WF $W(x, p)$ which for a quantum state ρ reads[67]

$$W(x,p) = \frac{1}{2\pi} \int_{-\infty}^{\infty} \mathrm{d}y\, e^{-ipy} \langle x + y|\rho|x - y\rangle. \tag{12}$$

WF shows a quasiprobability distribution over the phase space spanned by position x and momentum p and its negativity is a prerequisite of the non-classicallity of a quantum state. In Fig. 2b are WFs $W(0, p)$ of the mechanical oscillator computed for the same approximate states as in the panel (a). The WF of an ideal cubic phase state, i.e. the state given by Eq. (7) for $V(x) = x^3\gamma/(6\tau)$, reads[3,50]

$$W_{CPS}(x,p) \propto \mathrm{Ai}\left[\left(\frac{4}{\gamma}\right)^{1/3}(\gamma x^2 - p)\right], \tag{13}$$

where Ai(x) is the Airy function. This function with apparent non-Gaussian shape in the phase space exhibits fast oscillations reaching negative values in the positive momentum for any $\gamma > 0$. The WFs of the states obtained by application of the stroboscopic protocol approach the one of Eq. (8). Each of them exhibits areas with negative values which proves quantum non-Gaussian character of the resulting state. Moreover, with increased number of stroboscopic applications involved, the resulting approximate state corresponds to stronger nonlinearity. For the last curve where $M_T = 3$ we also show the result of an idealized instantaneous unitary application of an equal total nonlinearity by a cyan line with markers which is indistinguishable from the line for the approximate evolution. For this pair of curves we also have an estimate for the overlap $\mathrm{Tr}[\rho_{red}\rho_{cyan}]/\mathrm{Tr}[\rho_{cyan}^2] = 0.9877$. Despite an excellent overlap of the ideal and approximate WFs, the important resource, squeezing σ_3 shows a noticeable deviation from the ideal scenario. It is for this reason that we choose the squeezing σ_3 as the main figure of merit for the protocol.

DISCUSSION

In this article, we have proposed and theoretically analyzed a protocol to create a nonlinear motional state of the mechanical mode of an optomechanical system with controllable nonlinear mechanical potential. The method uses the possibility to apply the nonlinear potential to the motion of mechanical object in a stroboscopic way, twice per a period of oscillations. This way of application allows reducing the deteriorative effect of the free oscillations and approach the effect of pure action of nonlinear potential. In contrast to other methods of creating nonclassical states by a continuous evolution in presence of nonlinear terms in the Hamiltonian[68–70], our method allows approaching the states that approximate evolution according to the unitary $e^{iV(x)}$ where $V(x)$ is the nonlinear potential profile. We tested our method on a cubic nonlinearity $\propto \hat{x}^3$ though the method is applicable to a wide variety of nonlinearities. Our simulations prove that application of the protocol allows one to obtain the squeezing in the nonlinear quadrature below the shot-noise level even if the initial state of the particle is not pure. The nonlinear state created in a stroboscopic protocol clearly outperforms as a resource the vacuum for which the bound (11) holds. Moreover, the stroboscopic states approximate the one defined by Eq. (8) obtained in absence of the free rotation and thermal decoherence. We also verify that the stroboscopic application of the cubic nonlinear potential generates nonclassical states under conditions that are further from optimal than the ones of Fig. 2. In particular, we find that the heating rate H_m can be increased approximately 100-fold

until the curve $\sigma_3(\lambda)$ fails to overcome the vacuum boundary $1 + 2\lambda^2$. We are able to prove that when the duration of the application τ is increased tenfold such that the corresponding product $V(x)\tau$ remains constant, (that is, a less stiff potential is applied stroboscopically for proportionally longer time intervals), the resulting nonlinear state as well shows squeezing in σ_3. This proves robustness of the method to the two major imperfections.

We have shown the method to work for the parameters inspired by recent results demonstrated by the levitated optomechanical systems[71,72]. The optical trap with a cubic potential has been already used in the experiments[43,44]. Levitated systems[73], including electromechanical systems[74], have recently shown significant progress in the motional state cooling[35–37] and feedback-enhanced operation[34] which lays solid groundwork of the success of the proposed protocol. The authors of ref. [44] report the experimental realization of the potential $V(X) = \mu X^3/6$ with $\mu \approx 8k_B T \mu m^{-3}$, where $X = x\sqrt{\hbar/(2m\Omega_m)}$ is the dimensional displacement of the oscillator, m is its mass, k_B is the Boltzmann constant and T temperature. From this value we can make a very approximate estimate for the nonlinear gain $\gamma = \mu(\hbar/(2m\Omega_m))^{3/2}\tau \approx 1.2 \times 10^{-3}$ assuming duration $\tau = \pi/(50\Omega_m)$, temperature $T = 300$ K, frequency $\Omega_m = 2\pi \times 1$ kHz, and a mass $m = 4 \times 10^{-15}$ g of a silica nanoparticle of 70 nm radius.

Experimental implementation of the proposed method can guarantee preparation of a strongly non-Gaussian quantum motional state. Further analysis of such a state will require either a full state tomography or better suited well-tailored methods to prove the nonclassicality[75]. An analysis of the estimation of the nonlinear mechanical quadrature variance via pulsed optomechanical interaction can be found in ref. [66]. The optical read out can be improved using squeezed states of light[76]. This experimental step will open applications of the proposed method to other nonlinear potentials relevant for quantum computation[4,51,52,77], quantum thermodynamics[78,79] and quantum force sensing[80,81].

In our simulations, we focused solely on the dynamics of the mechanical mode and assumed the conventional optomechanical interaction absent. This interaction, well developed in recent years, provides a sufficiently rich toolbox that allows incorporation of the mechanical mode into the optical circuits of choice[9]. As an option, a prepared nonlinear state can be transferred to traveling light pulse[76] using optomechanical driving. In a more complicated scenario, one can add optomechanical interaction to the stroboscopic evolution to obtain even richer dynamics. A complete investigation of such dynamics, however, goes beyond the scope of the present research focused on the preparation of nonlinear motional states.

In parallel with the experimental verification, the stroboscopic method can be used to analyze other higher-order mechanical nonlinearities such as $V(x) \propto x^4$ or tilted double-well potentials required for tests of recently disputed quantum Landauer principle[82], counter-intuitive Fock state preparation[83] and approaching macroscopic superpositions[84–87].

METHODS

Tools of numerical simulations

The Eq. (6) approximates the damped evolution of an oscillator in a nonlinear potential by a sequence of individual stages of harmonic, nonlinear and damped harmonic evolution (see Fig. 1). Below we elaborate on how it is possible to simulate such dynamics using WF in the phase space, density matrix in position, momentum and Fock basis.

First, we evaluate the action of the nonlinearity during the stroboscopic pulse. While the nonlinearity is on, the Hamiltonian of the system reads

$$\hat{H} = \hat{H}_{HO} + V(\hat{x}) = \hat{H}_p + \hat{H}_x, \tag{14}$$

where $\hat{H}_p = \frac{\Omega_m}{4}\hat{p}^2$, and $\hat{H}_x = \frac{\Omega_m}{4}\hat{x}^2 + \frac{\gamma}{6}\hat{x}^3$.

Our important simulation tool is the STS (see ref. [48]) for $\hat{U}$

$$\hat{U}(t + \tau, t) = \left[\exp[-i(\hat{H}_{HO} + V(\hat{x}))\frac{\tau}{N}]\right]^N = \left[\hat{U}_{HO}(\frac{\tau}{N})\hat{U}_{NL}(\frac{\tau}{N}) + O\left(\left(\frac{\tau}{N}\right)^2\right)\right]^N, \tag{15}$$

where $\hat{U}_{HO}(\delta t) \equiv \exp(-iH_{HO}\delta t)$, $\hat{U}_{NL}(\delta t) \equiv \exp(-iV(x)\delta t)$, N is called the Trotter number. The accuracy of the approximation is, thereby, increasing with decreasing τ/N. Despite τ being now sufficiently large to take into account noticeable free rotation through an angle $\Omega_m\tau$ in the phase space, we still assume that τ is much shorter than the mechanical decoherence timescale, set by the heating rate H_m. This is well justified for the current experiments[33,36,37], also see Supplementary Note 2. The STS requires the summands forming the Hamiltonian to be self-adjoint which is not always the case of $V(x)$, in particular $V(x) \propto x^3$. We take the necessary precautions by considering such nonlinearities over only short time in a finite region of the phase space. Thus we cautiously take care of the quantum motional state being limited to this finite region. To further verify the correctness of numerics via STS, we cross-check it using numerical simulations in Fock-state basis.

Equation (14) shows the two possibilities to split the full Hamiltonian into summands to use the STS. We use these two possibilities to compute independently the mechanical state in order to verify the correctness of the STS in Supplementary Note 1.

First, we start from a squeezed thermal state $\rho(0)$, which has a representation by the WF in the phase space

$$W_{th}(x, p; n_0, s) = \frac{\exp\left(-\frac{1}{2}\left[\frac{(x/s)^2 + (ps)^2}{2n_0 + 1}\right]\right)}{2\pi(2n_0 + 1)}. \tag{16}$$

The WF corresponding to a quantum state ρ is defined[67] as

$$W(x, p) = \frac{1}{2\pi}\int_{-\infty}^{\infty} dy \, e^{-ipy}\langle x + y|\rho|x - y\rangle, \tag{17}$$

and the corresponding density matrix element can be obtained from the WF by an inverse Fourier transform. It is therefore possible to extend this approach to any $W(x, p)$ beyond the Gaussian states.

The evolution of a state ρ under action of a Hamiltonian proportional to a quadrature $\hat{q}$ can be straightforwardly computed in the basis of this quadrature, where it amounts to multiplication of density matrix elements with c-numbers:

$$\langle q|e^{-i\hat{H}_q(\hat{q})t}\rho e^{i\hat{H}_q(\hat{q})t}|q'\rangle = \langle q|\rho|q'\rangle e^{-i(H_q(q) - H_{q'}(q'))t}. \tag{18}$$

In particular, the nonlinear evolution reads

$$\langle x|\hat{U}_{NL}(\delta t)\rho\hat{U}_{NL}^\dagger(\delta t)|x'\rangle = \langle x|\rho|x'\rangle e^{-i[V(x) - V(x')]\delta t}. \tag{19}$$

The undamped harmonic evolution driven by $\hat{H}_{HO}$ can be represented by the rotation of WF in the phase space. A unitary rotation through an angle $\theta = \Omega_m\delta t$ in the phase space maps the initial WF $W(x, p; t)$ onto the final $W(x, p; t + \delta t)$ as

$$W(x, p; t + \delta t) = W(x \cos\theta - p \sin\theta, p \cos\theta + x \sin\theta; t). \tag{20}$$

The unitary transformation of the density matrix can be as well computed in the Fock state basis.

Finally, damped harmonic evolution of a high-Q harmonic oscillator over one half of an oscillation can also be evaluated in the phase space as a convolution of the initial WF $W(x, p; t)$ with a thermal kernel

$$W(x, p; t + \frac{\pi}{\Omega}) = \iint_{-\infty}^{\infty} du \, dv \, W_i(x - u, p - v; t)W_B(u, v), \tag{21}$$

where the expression for the kernel reads

$$W_B(u, v) = \frac{1}{2\pi\sigma_{th}}\exp\left[-\frac{u^2 + v^2}{2\sigma_{th}}\right], \tag{22}$$

with $\sigma_{th} = (2n_{th} + 1)2\pi\eta_m/\Omega_m$, where $n_{th} \approx k_B T/(\hbar\Omega_m)$ is the thermal occupation of the bath set by its temperature T. In terms of the heating rate H_m, $\sigma_{th} = 4\pi H_m/\Omega_m$. Equation (21) is obtained by solving the joint dynamics of the oscillator and bath followed by tracing out the latter. The detailed derivation of Eq. (21) can be found in Supplementary Note 2.

Using these techniques, one can evaluate the action of the map $\mathcal{N}$ defined by Eq. (6) on the state of the quantum oscillator. This yields the quantum state of the particle after one half of a mechanical oscillation. Repeatedly applying the same operations, one can obtain the state after multiple periods of the mechanical oscillations. Our purpose is then to

explore the limits of the achievable nonlinearities in optomechanical systems that are accessible now or are within reach.

DATA AVAILABILITY

The datasets generated and analyzed during the current study are available from the corresponding author on reasonable request.

REFERENCES

1. Braunstein, S. & van Loock, P. Quantum information with continuous variables. *Rev. Mod. Phys.* **77**, 513–577 (2005).
2. Lloyd, S. & Braunstein, S. L. Quantum computation over continuous variables. *Phys. Rev. Lett.* **82**, 1784–1787 (1999).
3. Gottesman, D., Kitaev, A. & Preskill, J. Encoding a qubit in an oscillator. *Phys. Rev. A* **64**, 012310 (2001).
4. Sefi, S. & van Loock, P. How to decompose arbitrary continuous-variable quantum operations. *Phys. Rev. Lett.* **107**, 170501 (2011).
5. Hastrup, J., Larsen, M. V., Neergaard-Nielsen, J. S., Menicucci, N. C. & Andersen, U. L. Unsuitability of cubic phase gates for non-Clifford operations on Gottesman-Kitaev-Preskill states. *Phys. Rev. A* **103**, 032409 (2021).
6. Meyer, N. et al. Resolved-sideband cooling of a levitated nanoparticle in the presence of laser phase noise. *Phys. Rev. Lett.* **123**, 153601 (2019).
7. Goldwater, D. et al. Levitated electromechanics: all-electrical cooling of charged nano- and micro-particles. *Quantum Sci. Technol.* **4**, 024003 (2019).
8. Vinante, A. et al. Ultralow mechanical damping with Meissner-levitated ferromagnetic microparticles. *Phys. Rev. Appl.* **13**, 064027 (2020).
9. Aspelmeyer, M., Kippenberg, T. J. & Marquardt, F. Cavity optomechanics. *Rev. Mod. Phys.* **86**, 1391–1452 (2014).
10. Aspelmeyer, M. et al. (eds.) *Cavity Optomechanics* (Springer, 2014).
11. Bowen, W. P. & Milburn, G. J. *Quantum Optomechanics* (CRC Press, 2015).
12. Khalili, F. Y. & Danilishin, S. L. Quantum optomechanics. In *Progress in Optics*, Vol. 61 (eds. Visser, T. D.) 113–236 (Elsevier, 2016).
13. Teufel, J. D. et al. Sideband cooling of micromechanical motion to the quantum ground state. *Nature* **475**, 359–363 (2011).
14. Chan, J. et al. Laser cooling of a nanomechanical oscillator into its quantum ground state. *Nature* **478**, 89–92 (2011).
15. Wollman, E. E. et al. Quantum squeezing of motion in a mechanical resonator. *Science* **349**, 952–955 (2015).
16. Pirkkalainen, J.-M., Damskägg, E., Brandt, M., Massel, F. & Sillanpää, M. A. Squeezing of quantum noise of motion in a micromechanical resonator. *Phys. Rev. Lett.* **115**, 243601 (2015).
17. Riedinger, R. et al. Remote quantum entanglement between two micromechanical oscillators. *Nature* **556**, 473–477 (2018).
18. Ockeloen-Korppi, C. F. et al. Stabilized entanglement of massive mechanical oscillators. *Nature* **556**, 478–482 (2018).
19. Barker, P. F. & Shneider, M. N. Cavity cooling of an optically trapped nanoparticle. *Phys. Rev. A* **81**, 023826 (2010).
20. Chang, D. E. et al. Cavity opto-mechanics using an optically levitated nanosphere. *Proc. Natl Acad. Sci.* **107**, 1005–1010 (2010).
21. Romero-Isart, O. et al. Optically levitating dielectrics in the quantum regime: theory and protocols. *Phys. Rev. A* **83**, 013803 (2011).
22. Millen, J. & Stickler, B. A. Quantum experiments with microscale particles. *Contemp Phys.* **61**, 155–168 (2020).
23. Moore, D. C., Rider, A. D. & Gratta, G. Search for millicharged particles using optically levitated microspheres. *Phys. Rev. Lett.* **113**, 251801 (2014).
24. Ranjit, G., Cunningham, M., Casey, K. & Geraci, A. A. Zeptonewton force sensing with nanospheres in an optical lattice. *Phys. Rev. A* **93**, 053801 (2016).
25. Gieseler, J., Novotny, L. & Quidant, R. Thermal nonlinearities in a nanomechanical oscillator. *Nat. Phys.* **9**, 806–810 (2013).
26. Ricci, F. et al. Optically levitated nanoparticle as a model system for stochastic bistable dynamics. *Nat. Commun.* **8**, 15141 (2017).
27. Gieseler, J. & Millen, J. Levitated nanoparticles for microscopic thermodynamics - a review. *Entropy* **20**, 326 (2018).
28. Romero-Isart, O. Quantum superposition of massive objects and collapse models. *Phys. Rev. A* **84**, 052121 (2011).
29. Bateman, J., Nimmrichter, S., Hornberger, K. & Ulbricht, H. Near-field interferometry of a free-falling nanoparticle from a point-like source. *Nat. Commun.* **5**, 4788 (2014).
30. Goldwater, D., Paternostro, M. & Barker, P. F. Testing wave-function-collapse models using parametric heating of a trapped nanosphere. *Phys. Rev. A* **94**, 010104 (2016).
31. Bose, S. et al. Spin entanglement witness for quantum gravity. *Phys. Rev. Lett.* **119**, 240401 (2017).
32. Marletto, C. & Vedral, V. Gravitationally induced entanglement between two massive particles is sufficient evidence of quantum effects in gravity. *Phys. Rev. Lett.* **119**, 240402 (2017).
33. Jain, V. et al. Direct measurement of photon recoil from a levitated nanoparticle. *Phys. Rev. Lett.* **116**, 243601 (2016).
34. Vovrosh, J. et al. Parametric feedback cooling of levitated optomechanics in a parabolic mirror trap. *JOSA B* **34**, 1421–1428 (2017).
35. Windey, D. et al. Cavity-based 3D cooling of a levitated nanoparticle via coherent scattering. *Phys. Rev. Lett.* **122**, 123601 (2019).
36. Delić, U. et al. Cavity cooling of a levitated nanosphere by coherent scattering. *Phys. Rev. Lett.* **122**, 123602 (2019).
37. Delić, U. et al. Cooling of a levitated nanoparticle to the motional quantum ground state. *Science* **367**, 892–895 (2020).
38. Rudolph, H., Hornberger, K. & Stickler, B. A. Entangling levitated nanoparticles by coherent scattering. *Phys. Rev. A* **101**, 011804 (2020).
39. Rakhubovsky, A. A. et al. Detecting nonclassical correlations in levitated cavity optomechanics. *Phys. Rev. Appl.* **14**, 054052 (2020).
40. Bérut, A. et al. Experimental verification of Landauer's principle linking information and thermodynamics. *Nature* **483**, 187–189 (2012).
41. Ryabov, A., Zemánek, P. & Filip, R. Thermally induced passage and current of particles in a highly unstable optical potential. *Phys. Rev. E* **94**, 042108 (2016).
42. Ornigotti, L., Ryabov, A., Holubec, V. & Filip, R. Brownian motion surviving in the unstable cubic potential and the role of Maxwell's demon. *Phys. Rev. E* **97**, 032127 (2018).
43. Šiler, M. et al. Thermally induced micro-motion by inflection in optical potential. *Sci. Rep.* **7**, 1697 (2017).
44. Šiler, M. et al. Diffusing up the hill: dynamics and equipartition in highly unstable systems. *Phys. Rev. Lett.* **121**, 230601 (2018).
45. Konopik, M., Friedenberger, A., Kiesel, N. & Lutz, E. Nonequilibrium information erasure below kTln2. *Europhys. Lett.* **131**, 60004 (2020).
46. Braginsky, V. B., Vorontsov, Y. I. & Khalili, F. Y. Optimal quantum measurements in detectors of gravitation radiation. *JETP Lett.* **27**, 276 (1978).
47. Caves, C. M., Thorne, K. S., Drever, R. W. P., Sandberg, V. D. & Zimmermann, M. On the measurement of a weak classical force coupled to a quantum-mechanical oscillator. I. Issues of principle. *Rev. Mod. Phys.* **52**, 341–392 (1980).
48. Suzuki, M. Generalized Trotter's formula and systematic approximants of exponential operators and inner derivations with applications to many-body problems. *Comm. Math. Phys.* **51**, 183–190 (1976).
49. Bartlett, S. D. & Sanders, B. C. Universal continuous-variable quantum computation: Requirement of optical nonlinearity for photon counting. *Phys. Rev. A* **65**, 042304 (2002).
50. Ghose, S. & Sanders, B. C. Non-Gaussian ancilla states for continuous variable quantum computation via Gaussian maps. *J. Mod. Opt.* **54**, 855–869 (2007).
51. Miyata, K. et al. Implementation of a quantum cubic gate by an adaptive non-Gaussian measurement. *Phys. Rev. A* **93**, 022301 (2016).
52. Marek, P. et al. General implementation of arbitrary nonlinear quadrature phase gates. *Phys. Rev. A* **97**, 022329 (2018).
53. Sivak, V. et al. Kerr-free three-wave mixing in superconducting quantum circuits. *Phys. Rev. Appl.* **11**, 054060 (2019).
54. Brunelli, M., Malz, D., Schliesser, A. & Nunnenkamp, A. Stroboscopic quantum optomechanics. *Phys. Rev. Res.* **2**, 023241 (2020).
55. Corbitt, T. et al. An all-optical trap for a Gram-Scale mirror. *Phys. Rev. Lett.* **98**, 150802 (2007).
56. Sridaran, S. & Bhave, S. A. Electrostatic actuation of silicon optomechanical resonators. *Opt. Express* **19**, 9020–9026 (2011).
57. Mason, D., Chen, J., Rossi, M., Tsaturyan, Y. & Schliesser, A. Continuous force and displacement measurement below the standard quantum limit. *Nat. Phys.* **1** (2019).
58. Lamata, L., Parra-Rodriguez, A., Sanz, M. & Solano, E. Digital-analog quantum simulations with superconducting circuits. *Adv. Phys. X* **3**, 1457981 (2018).
59. Lougovski, P., Lamata, L., Solano, E., Sanz, M. & Parra-Rodriguez, A. Digital-analog quantum computation. *Phys. Rev. A* **101**, 022305 (2020).
60. Weinbub, J. & Ferry, D. K. Recent advances in Wigner function approaches. *Appl. Phys. Rev.* **5**, 041104 (2018).
61. Yoshikawa, J.-i, Makino, K., Kurata, S., van Loock, P. & Furusawa, A. Creation, storage, and on-demand release of optical quantum states with a negative wigner function. *Phys. Rev. X* **3**, 041028 (2013).
62. Kienzler, D. et al. Observation of quantum interference between separated mechanical oscillator wave packets. *Phys. Rev. Lett.* **116**, 140402 (2016).
63. Wang, C. et al. A Schrödinger cat living in two boxes. *Science* **352**, 1087–1091 (2016).

64. Johnson, K. G., Wong-Campos, J. D., Neyenhuis, B., Mizrahi, J. & Monroe, C. Ultrafast creation of large Schrödinger cat states of an atom. *Nat. Commun.* **8**, 697 (2017).
65. Yukawa, M. et al. Emulating quantum cubic nonlinearity. *Phys. Rev. A* **88**, 053816 (2013).
66. Moore, D. W., Rakhubovsky, A. A. & Filip, R. Estimation of squeezing in a nonlinear quadrature of a mechanical oscillator. *New J. Phys.* **21**, 113050 (2019).
67. Schleich, W. P. Quantum Optics in Phase Space (John Wiley & Sons, 2011).
68. Ballentine, L. E. & McRae, S. M. Moment equations for probability distributions in classical and quantum mechanics. *Phys. Rev. A* **58**, 1799–1809 (1998).
69. Brizuela, D. Classical and quantum behavior of the harmonic and the quartic oscillators. *Phys. Rev. D* **90**, 125018 (2014).
70. Brizuela, D. Statistical moments for classical and quantum dynamics: formalism and generalized uncertainty relations. *Phys. Rev. D* **90**, 085027 (2014).
71. Kiesel, N. et al. Cavity cooling of an optically levitated submicron particle. *Proc. Natl Acad. Sci. USA* **110**, 14180–14185 (2013).
72. Magrini, L. et al. Near-field coupling of a levitated nanoparticle to a photonic crystal cavity. *Optica* **5**, 1597–1602 (2018).
73. Millen, J. & Stickler, B. A. Quantum experiments with microscale particles. *Contemp. Phys.* **61**, 155–168, https://doi.org/10.1080/00107514.2020.1854497 (2020).
74. Martinetz, L., Hornberger, K., Millen, J., Kim, M. S. & Stickler, B. A. Quantum electromechanics with levitated nanoparticles. *npj Quantum Inf.* **6**, 1–8 (2020).
75. Vanner, M. R., Pikovski, I. & Kim, M. S. Towards Optomechanical Quantum State Reconstruction of Mechanical Motion. *Ann. Phys.* **527**, 15–26 (2015).
76. Filip, R. & Rakhubovsky, A. A. Transfer of non-Gaussian quantum states of mechanical oscillator to light. *Phys. Rev. A* **92**, 053804 (2015).
77. Marek, P., Filip, R. & Furusawa, A. Deterministic implementation of weak quantum cubic nonlinearity. *Phys. Rev. A* **84**, 053802 (2011).
78. Zhang, K., Bariani, F. & Meystre, P. Quantum optomechanical heat engine. *Phys. Rev. Lett.* **112**, 150602 (2014).
79. Dechant, A., Kiesel, N. & Lutz, E. All-optical nanomechanical heat engine. *Phys. Rev. Lett.* **114**, 183602 (2015).
80. Rugar, D., Budakian, R., Mamin, H. J. & Chui, B. W. Single spin detection by magnetic resonance force microscopy. *Nature* **430**, 329–332 (2004).
81. Degen, C. L., Poggio, M., Mamin, H. J., Rettner, C. T. & Rugar, D. Nanoscale magnetic resonance imaging. *Proc. Natl Acad. Sci. USA* **106**, 1313–1317 (2009).
82. Miller, H. J. D., Guarnieri, G., Mitchison, M. T. & Goold, J. Quantum fluctuations hinder finite-time information erasure near the Landauer limit. *Phys. Rev. Lett.* **125**, 160602 (2020).
83. Simón, M. A., Palmero, M., Martinez-Garaot, S. & Muga, J. G. Trapped-ion Fock-state preparation by potential deformation. *Phys. Rev. Res.* **2**, 023372 (2020).
84. Abdi, M., Degenfeld-Schonburg, P., Sameti, M., Navarrete-Benlloch, C. & Hartmann, M. J. Dissipative optomechanical preparation of macroscopic quantum superposition states. *Phys. Rev. Lett.* **116**, 233604 (2016).
85. Gerry, C. & Knight, P. Introductory Quantum Optics (Cambridge University Press, 2004).
86. Palomaki, T. A., Teufel, J. D., Simmonds, R. W. & Lehnert, K. W. Entangling Mechanical Motion with Microwave Fields. *Science* **342**, 710–713 (2013).
87. Hall, B. C. *Quantum Theory for Mathematicians* (Springer Science & Business Media, 2013).

AUTHOR CONTRIBUTIONS

R.F. conceived the theoretical idea. A.A.R. performed the numerical computations. Both authors participated in writing the manuscript.

COMPETING INTERESTS

The authors declare no competing interests.

ADDITIONAL INFORMATION

Supplementary information The online version contains supplementary material available at https://doi.org/10.1038/s41534-021-00453-8.

Correspondence and requests for materials should be addressed to A.A.R.

Reprints and permission information is available at http://www.nature.com/reprints

Publisher's note Springer Nature remains neutral with regard to jurisdictional claims in published maps and institutional affiliations.